

## Heme–Heme Interactions in the Cytochrome $b_6f$ Complex: EPR Spectroscopy and Correlation with Structure

Anna I. Zatsman,<sup>†</sup> Huamin Zhang,<sup>‡</sup> William A. Gundersen,<sup>†</sup> William A. Cramer,<sup>‡</sup> and Michael P. Hendrich<sup>\*†</sup>

*Department of Chemistry, Carnegie Mellon University, Pittsburgh, Pennsylvania 15213, and  
Department of Biological Sciences, Purdue University, West Lafayette, Indiana 47907*

Received August 9, 2006; E-mail: hendrich@andrew.cmu.edu

The 220 kDa dimeric cytochrome  $b_6f$  complex of oxygenic photosynthesis provides the “linear” or “noncyclic” electronic connection between the two reaction centers photosystems I and II that are, respectively, coupled to NADP<sup>+</sup> reduction and oxygen evolution.<sup>1</sup> The  $b_6f$  complex has also been implicated in the “cyclic” electron transport pathway connected to photosystem I that regulates the ratio of ATP and NADPH without any net electron transfer.<sup>2</sup> The electron transport functions of the  $b_6f$  complex are coupled to proton transfer and generation of a trans-membrane proton electrochemical gradient, by mechanisms similar to those of the cytochrome  $bc_1$  complex of the respiratory chain and the photosynthetic bacteria,<sup>3</sup> whose protein core is similar to that of the  $b_6f$  complex.<sup>4</sup> Prior to X-ray crystal structure analysis, each monomeric unit of the complex was known to contain six bound prosthetic groups, three hemes ( $f$ , two hemes  $b$ ,  $b_p$  and  $b_n$ ), one [2Fe-2S] cluster, and one molecule each of chlorophyll  $a$ <sup>5,6</sup> and  $\beta$ -carotene.<sup>6</sup>

Crystal structure analysis of the  $b_6f$  complex from a green alga<sup>7</sup> and a thermophilic cyanobacterium<sup>8</sup> revealed the presence of an additional heme  $c_n$ , previously detected spectrophotometrically,<sup>9</sup> which is covalently bound on the electrochemically negative ( $n$ )-side of the complex at a site very close to a  $b$ -heme ( $b_n$ ). Only one axial ligand of heme  $c_n$ , a water molecule, has been reported. The water is hydrogen bonded to the  $O$  atom of a propionate of heme  $b_n$  (Figure 1). The presence of heme  $c_n$  is a feature of the structure of the  $b_6f$  complex that is unique compared to the  $bc_1$  complex. In spite of the small distance of separation between the two hemes, it has been implied previously that hemes  $b_n$  and  $c_n$  are electronically independent.<sup>1,7,8</sup> This assumption is examined in the present work.

Many EPR studies of the cytochrome  $b_6f$  complex have been reported over the past 25 years.<sup>10–13</sup> In all these studies, signals with  $g > 4.3$  were attributed either to an impurity species, to a low-spin heme that lost an axial histidine, or to a mixture of isolated high-spin species. Here, we demonstrate that all signals above  $g = 4.3$  are in fact associated with a spin interaction between heme  $b_n$  and heme  $c_n$ . No significant amount of isolated high-spin heme is present in native preparations. Furthermore, the addition of quinone analog NQNO (2- $n$ -nonyl-4-hydroxyquinoline  $N$ -oxide) causes a significant change in signals, but the two hemes remain spin-coupled.

X- and Q-band EPR spectra of the native cytochrome  $b_6f$  complex and simulations are shown in Figure 2 with magnetic fields shifted to give equal  $g$ -value scales. The X-band data are shown for conventional perpendicular orientation of magnetic field  $\mathbf{B}_1$  with respect to the static field  $\mathbf{B}$  (Figure 2A) and for parallel orientation of these two fields (Figure 2E). The signal at  $g = 4.3$  is due to an adventitious Fe(III) impurity with a concentration of less than 5% of the protein concentration. The signal at  $g = 3.51$  is from

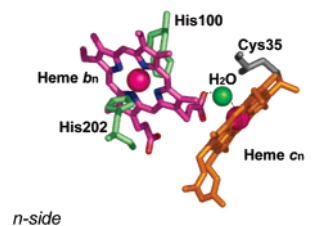


**Figure 1.** Hemes  $b_n$  and  $c_n$  near the electrochemically negative side ( $n$ ) of the cytochrome  $b_6f$  complex.

cytochrome  $f$ ,<sup>14</sup> and the simulation (Figure 2C) indicates that approximately 60% of it is reduced. The signal at  $g = 3.68$  is from low-spin heme  $b_p$ , and the simulation of this signal (Figure 2B) indicates a spin concentration comparable to the protein concentration. Previously, this signal was thought to be from both  $b$  hemes of the complex.<sup>12</sup> However, the signal quantitation and presence of the spin interacting system discussed next both indicate that the  $g = 3.68$  signal originates only from the  $b_p$  heme.

The X- and Q-band spectra for  $\mathbf{B}_1 \perp \mathbf{B}$  show many signals for  $g > 4.3$  which have frequency-dependent  $g$ -values. For half-integer spin systems with large zero-field energies, this and the observation of the parallel-mode signal (Figure 2E) indicate the presence of spin interactions. None of the signals above  $g = 4.3$  can be attributed to a significant fraction of an isolated (noninteracting) heme species. The simulations D, F, and H shown in Figure 2 are calculated for a high-spin heme ( $S_1 = 5/2$ ) exchange coupled to a low-spin heme ( $S_2 = 1/2$ ), all using the same set of parameters given in the figure capture. The fit requires that the  $g$ -tensor of heme  $b_n$  (low-spin) has one large  $g$ -value near 3.7 in a direction aligned with the in-plane  $g$ -values of heme  $c_n$  (high-spin). This is consistent with the structure of the cyt  $b_6f$  complex which shows a crossed imidazole plane configuration for heme  $b_n$  (Figure 1). This crossed configuration results in one  $g$ -value greater than 3.2, aligned near the direction of the heme normal.<sup>15</sup> Furthermore, the structure shows that the hemes  $b_n$  and  $c_n$  planes are nearly orthogonal; thus, the large  $g$ -value of heme  $b_n$  will be aligned with the in-plane  $g$ -values of heme  $c_n$ .

We have not yet found a simulation parameter set which correctly positions all resonances. The parameter space is large, including the exact magnitudes and relative orientations of  $g$ -tensors and possible anisotropy of the  $\mathbf{J}$ -tensor. Nevertheless, many of the spectral features match in all three sets of data. In particular, the parallel mode simulation (Figure 2F) matches the experimental spectrum reasonably well, and from this match we determine that the spin concentration of the high-spin/low-spin heme pair is in approximate agreement with the protein concentration. The additional resonances not observed in the simulations may also be due to a second conformation of the high-spin/low-spin pair. Most notably, we have been unable to simulate a doublet feature in a

<sup>†</sup> Carnegie Mellon University.

<sup>‡</sup> Purdue University.

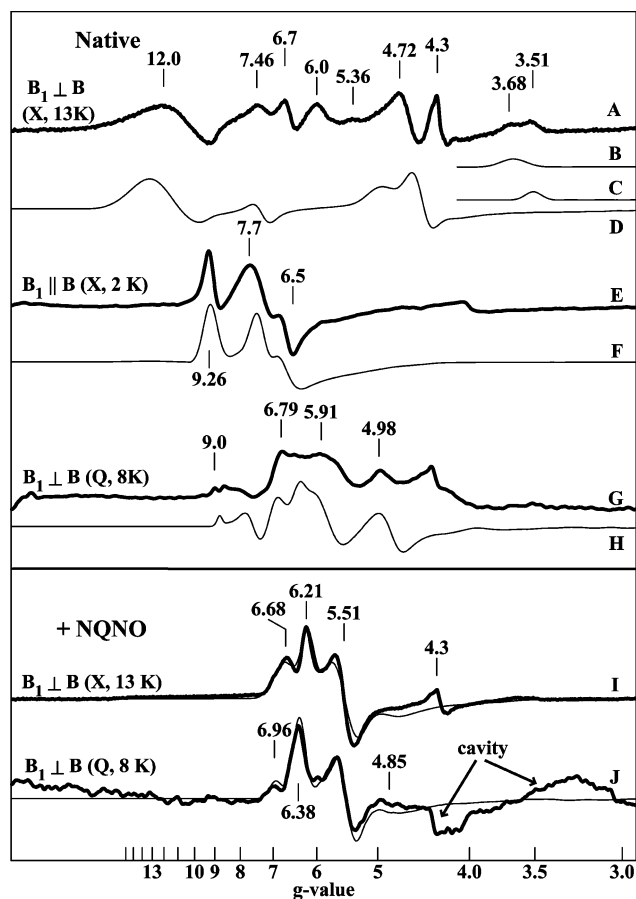


**Figure 2.** Multifrequency EPR spectra (thick lines, conditions as listed) and simulations (thin lines) of native cytochrome  $b_6f$  complex ( $\sim 0.1$  mM, pH 7.5) from spinach (A–H), and with excess NQNO (I, J). (B) Simulation of low-spin heme  $b_7$  ( $g = 0.63, 1.53, 3.68$ ), (C) low-spin heme  $f$  ( $g = 0.78, 1.70, 3.51$ ). The simulations D, F, and H are for an exchanged-coupled system:  $S_1 = 5/2, S_2 = 1/2, g_1 = 1.98, D_1 = 7 \text{ cm}^{-1}, E/D_1 = 0.033, g_2 = 0.4, 1.6, 3.7, J_{\text{iso}} = 0.074 \text{ cm}^{-1}, S_2$  Euler rotation ( $0^\circ, 90^\circ, 90^\circ$ ). The simulations (I, J) of the NQNO samples are overlaid on data and are composed of two species: (i) an exchanged-coupled system  $S_i = 5/2, S_2 = 1/2, g_1 = 1.98, D_1 = 7 \text{ cm}^{-1}, E/D_1 = 0.02, g_2 = 0.9, 1.7, 3.5, J = 0.0035, 0.0085, 0.007 \text{ cm}^{-1}, S_2$  Euler rotation ( $0^\circ, 90^\circ, 90^\circ$ ) and (ii) an isolated high-spin heme species with  $g = 6.96, 4.85$  ( $E/D = 0.045$ ). Signals from the cavity background are as indicated.

Q-band spectrum near  $g = 9$  with inclusion of  $J$ -anisotropy and a dipole interaction.

Heme–heme interactions have been previously characterized in other multiheme proteins, such as the octaheme hydroxylamine oxidoreductase<sup>16</sup> and tetraheme cytochrome  $c_554$ .<sup>17</sup> In those proteins, the porphyrin planes of interacting hemes are approximately parallel, allowing for a direct  $\pi$ – $\pi$  overlap of porphyrin orbitals. However, in cyt  $b_6f$ , the porphyrin planes of hemes  $b_n$  and  $c_n$  are nearly orthogonal. Thus, the spin interaction is likely to be via the H-bond of the bridging water molecule rather than  $\pi$ – $\pi$  overlap.

Heme  $c_n$  is unique in nature in having no protein ligands coordinating axial to the heme. Thus, we expect that small molecules such as cyanide would bind to heme  $c_n$ . Surprisingly, the addition of  $\text{CN}^-$  at pH 8.5, or its hydrophobic analog butyl isocyanide, had only minor effects on the EPR spectra. In contrast, the addition of the quinone analog NQNO showed a significant spectral change. NQNO is a  $Q_n$  pocket inhibitor which shifts the

potential of heme  $c_n$  by approximately  $-200$  mV.<sup>18</sup> The X- and Q-band spectra of cyt  $b_6f$  treated with an excess of NQNO are shown in Figure 2I and J. Here again, the  $g$ -values of the signals depend on the microwave frequency, indicating spin interactions are still present (the parallel mode signal vanishes owing to the weaker interaction). The simulations shown (thin lines on data) are composed of two species, a weakly interacting high-spin/low-spin heme pair and a minority isolated high-spin species. The spin-coupled signals of the native spectrum are nearly quantitatively converted to the signals of the new spin-interacting system. Importantly, the  $E/D$  value for heme  $c_n$  changes from 0.033 to 0.02, and the strength of the coupling in the presence of NQNO is significantly weaker than that of the native complex. The change in  $E/D$  indicates binding of NQNO in close proximity, possibly as an axial ligand, to the heme  $c_n$ . The 10-fold decrease in the exchange interaction suggests a weakening of the H-bond between the bridging water molecule and propionate O atom. The minority species is an isolated high-spin heme ( $g = 6.96, 4.85; E/D = 0.045$ ) which quantifies to  $<20\%$  of the protein concentration. This species is not evident in the native sample, suggesting that it is due to a second binding mode of NQNO to heme  $c_n$ .

We have demonstrated the presence of an electronic exchange interaction between hemes  $b_n$  and  $c_n$  and shown that a quinone analog binds at or near to heme  $c_n$ . The electronic coupling implies that the heme  $b_n/c_n$  pair could function as a unit to facilitate 2-electron reduction of plastoquinone without generation of an energetically unfavorable semiquinone intermediate.

**Acknowledgment.** The research was supported by grants from NIH: Grants GM-077387 (M.P.H.) and GM-38323 (W.A.C.).

**Supporting Information Available:** Experimental procedures, simulation methods, and energy level diagrams. This material is available free of charge via the Internet at <http://pubs.acs.org>.

## References

- (1) Cramer, W. A.; Zhang, H.; Yan, J.; Kurisu, G.; Smith, J. L. *Annu. Rev. Biochem.* **2006**, *75*, 769–790.
- (2) Zhang, H.; Whitelegge, J. P.; Cramer, W. A. *J. Biol. Chem.* **2001**, *276*, 38159–38165.
- (3) Berry, E. A.; Guergova-Kuras, M.; Huang, L.-S.; Crofts, A. R. *Annu. Rev. Biochem.* **2000**, *69*, 1005–1075.
- (4) Widger, W. R.; Cramer, W. A.; Herrmann, R. G.; Trebst, A. *Proc. Natl. Acad. Sci. U.S.A.* **1984**, *81*, 674–678.
- (5) Huang, D.; Everly, R. M.; Cheng, R. H.; Heymann, J. B.; Schaeffer, H.; Sled, V.; Ohnishi, T.; Baker, T. S.; Cramer, W. A. *Biochemistry* **1994**, *33*, 4401–4409.
- (6) Zhang, H.; Huang, D.; Cramer, W. A. *J. Biol. Chem.* **1999**, *274*, 1581–1587.
- (7) Stroebel, D.; Choquet, Y.; Popot, J.-L.; Picot, D. *Nature* **2003**, *426*, 413–418.
- (8) Kurisu, G.; Zhang, H.; Smith, J. L.; Cramer, W. A. *Science* **2003**, *302*, 1009–1014.
- (9) Joliot, P.; Joliot, A. *Biochim. Biophys. Acta* **1988**, *933*, 319–333.
- (10) Salerno, J. C.; McGill, J. W.; Gerstle, G. C. *FEBS Lett.* **1983**, *162*, 257–261.
- (11) Nitschke, W.; Hauska, G. *Biochim. Biophys. Acta* **1987**, *892*, 314–319.
- (12) Schunemann, V.; Trautwein, A. X.; Illerhaus, J.; Haehnel, W. *Biochemistry* **1999**, *38*, 8981–8991.
- (13) Zhang, H.; Primak, A.; Cape, J.; Bowman, M. K.; Kramer, D. M.; Cramer, W. A. *Biochemistry* **2004**, *43*, 16329–16336.
- (14) Rigby, S. E. J.; Moore, G. R.; Gray, J. C.; Gadsby, P. M. A.; George, S. J.; Thomson, A. J. *Biochem. J.* **1988**, *256*, 571–577.
- (15) Shokhirev, N. V.; Walker, F. A. *J. Am. Chem. Soc.* **1998**, *120*, 981–990.
- (16) Hendrich, M. P.; Petasis, D.; Arciero, D. M.; Hooper, A. B. *J. Am. Chem. Soc.* **2001**, *123*, 2997–3005.
- (17) Upadhyay, A. K.; Petasis, D. T.; Arciero, D. M.; Hooper, A. B.; Hendrich, M. P. *J. Am. Chem. Soc.* **2003**, *125*, 1738–1747.
- (18) Alric, J.; Pierre, Y.; Picot, D.; Laverge, J.; Rappaport, F. *Proc. Natl. Acad. Sci. U.S.A.* **2005**, *102*, 15860–15865.

JA065798M